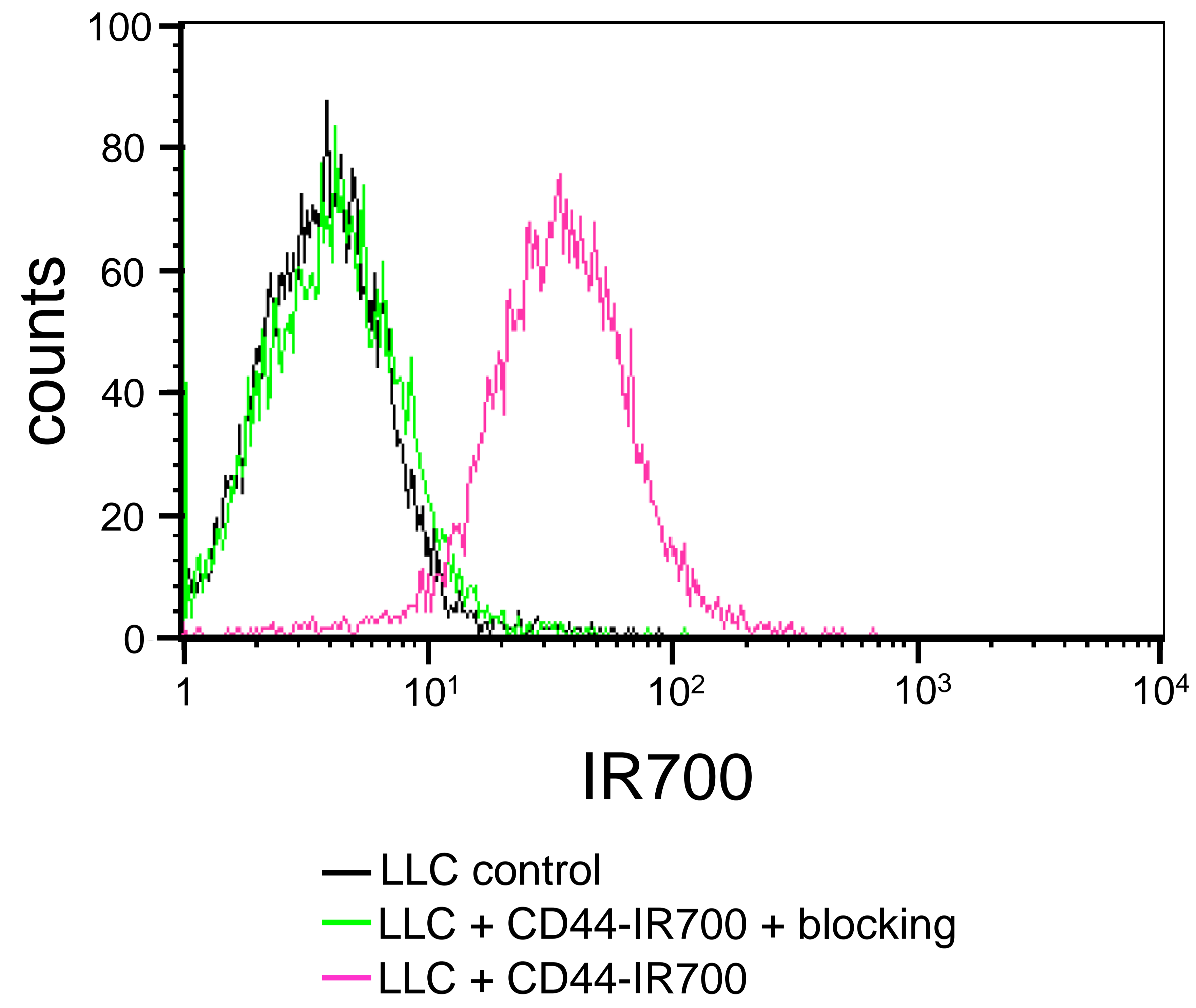
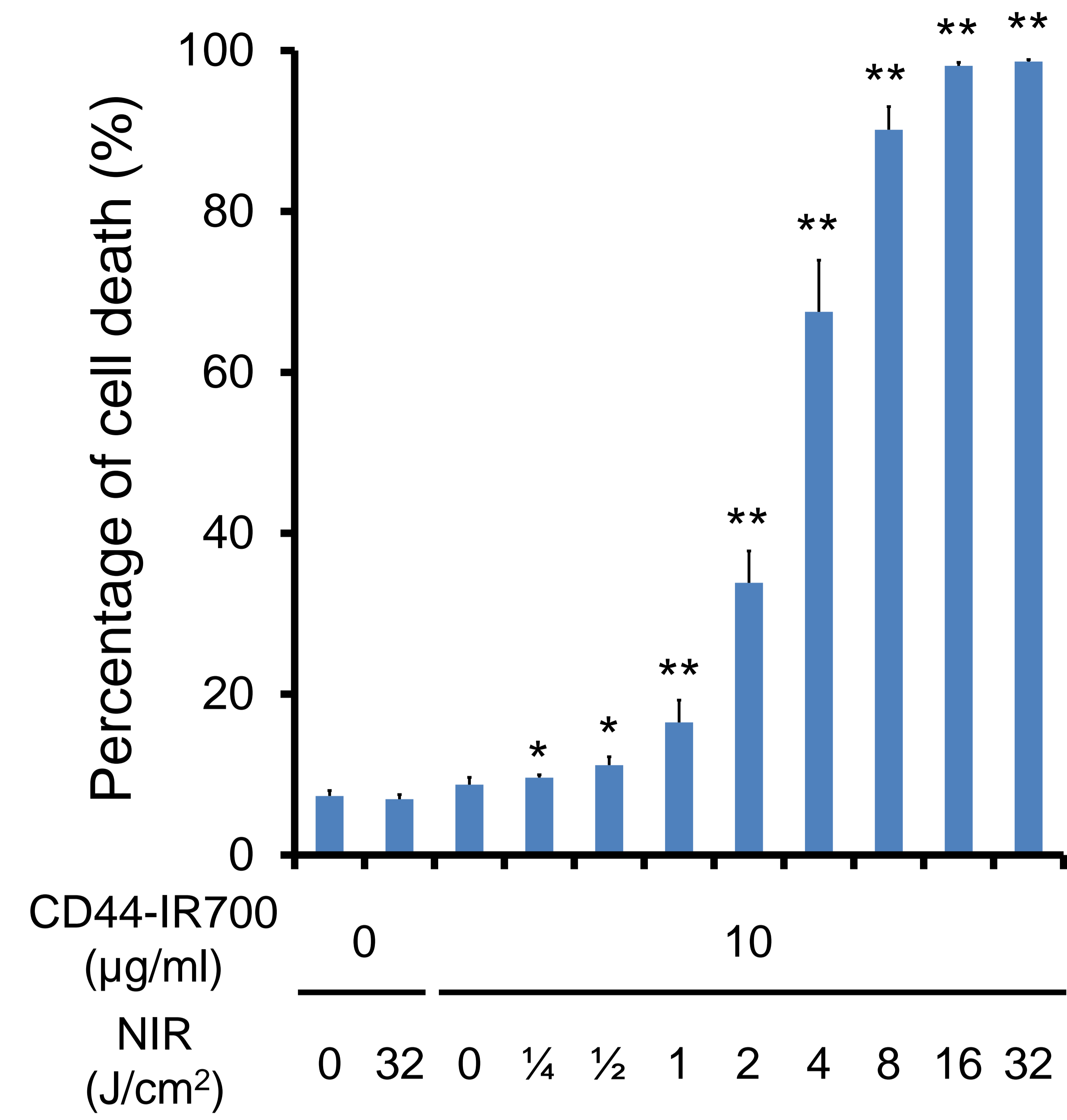


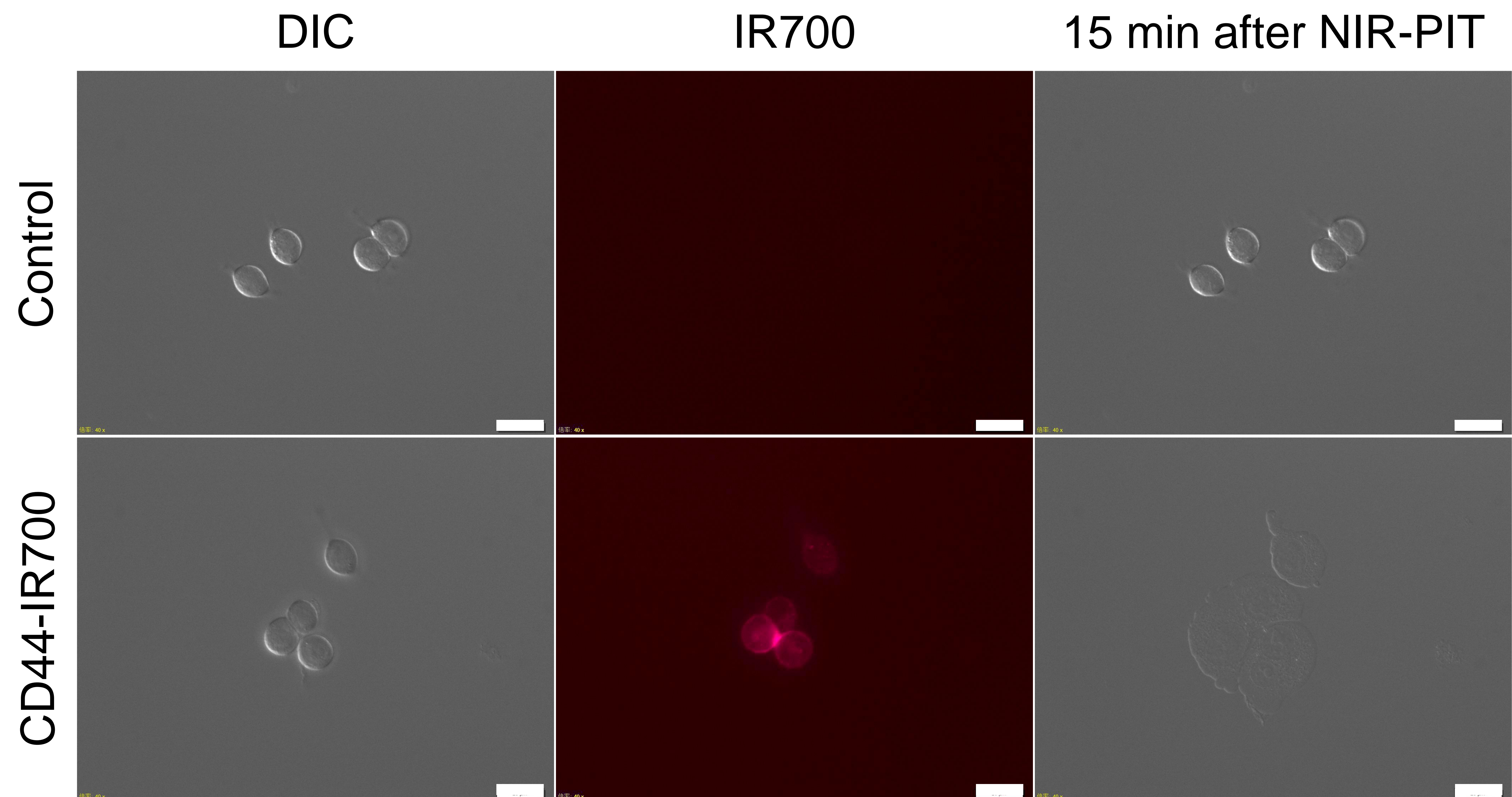
A



C



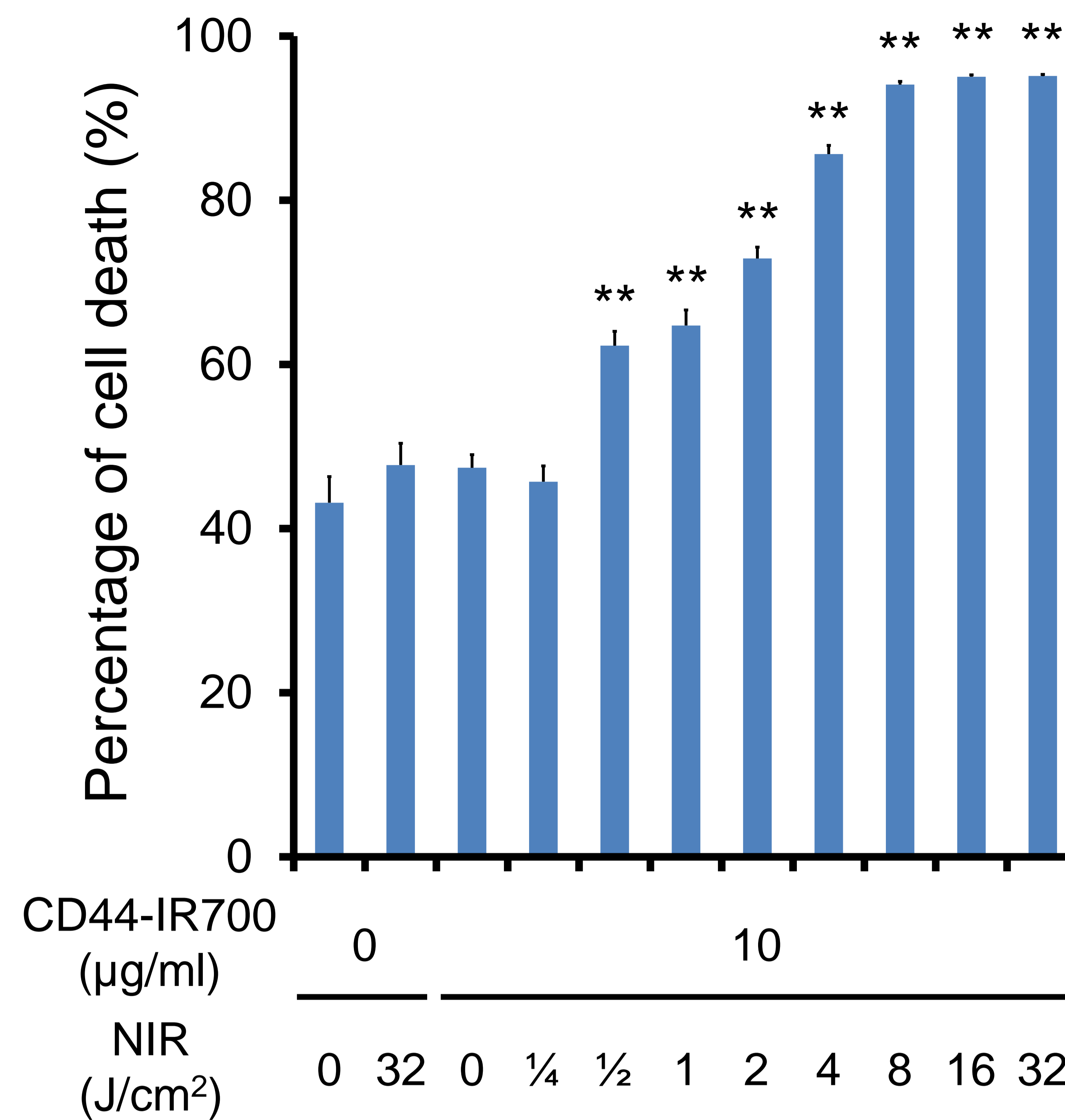
B



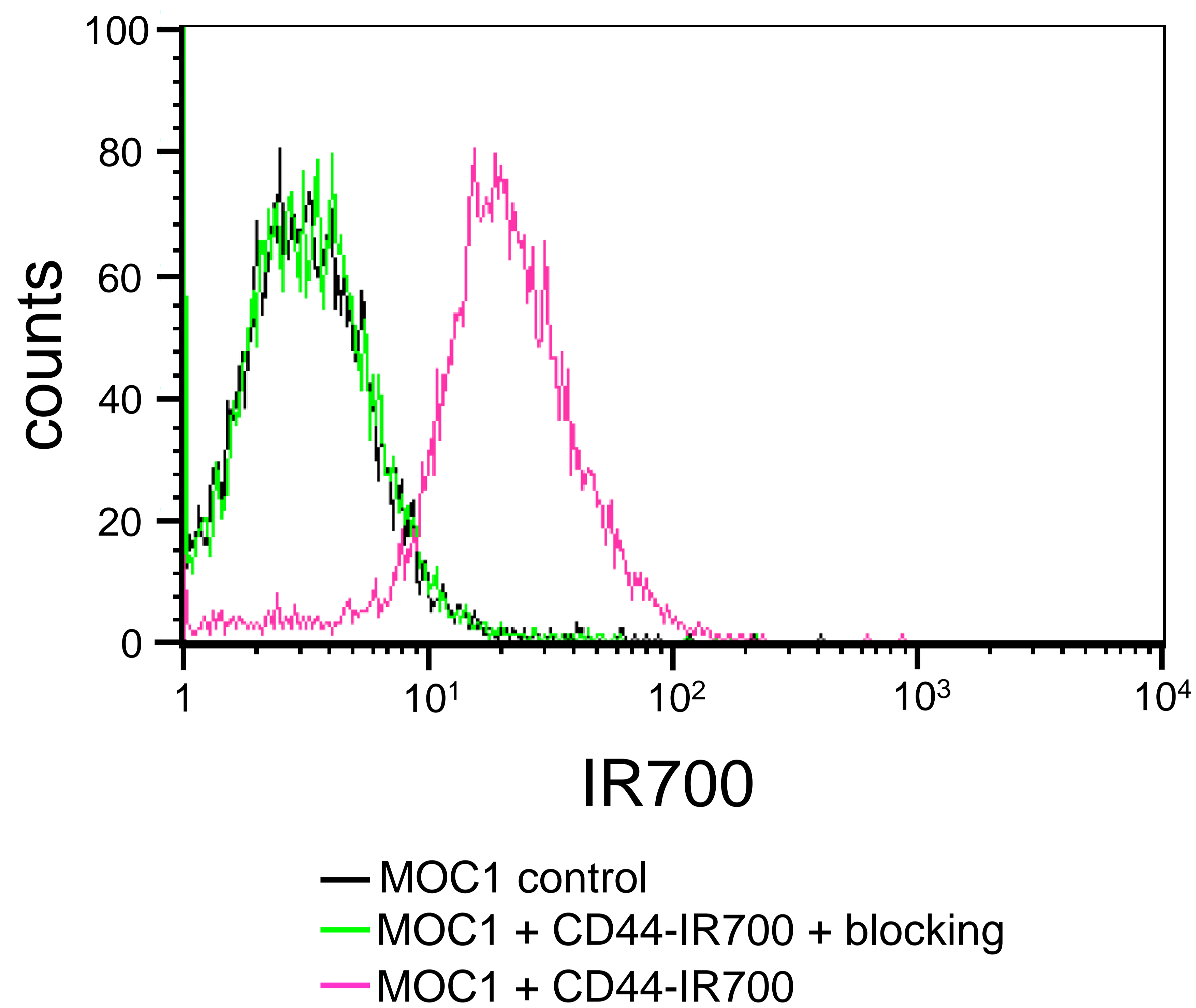
Supplementary Figure 1. Confirmation of CD44 expression as a target for NIR-PIT in LLC cells and evaluation of *in vitro* NIR-PIT.

(A) Expression of cell surface CD44 in LLC cells was examined with flow cytometry. CD44 blocking antibody was added to some wells to validate specific staining. Representative histograms shown. (B) Differential interference contrast (DIC) and fluorescence microscopy images of LLC cells. Change in LLC cellular architecture following 15 min of NIR light exposure shown. Scale bars = 20 μm . (C) Membrane permeability of LLC cells, as measured by propidium iodide (PI) staining, after labeling with CD44-IR700 and treatment with NIR-light (n = 5, * $p < 0.05$, ** $p < 0.01$, vs untreated control, by Student's t test).

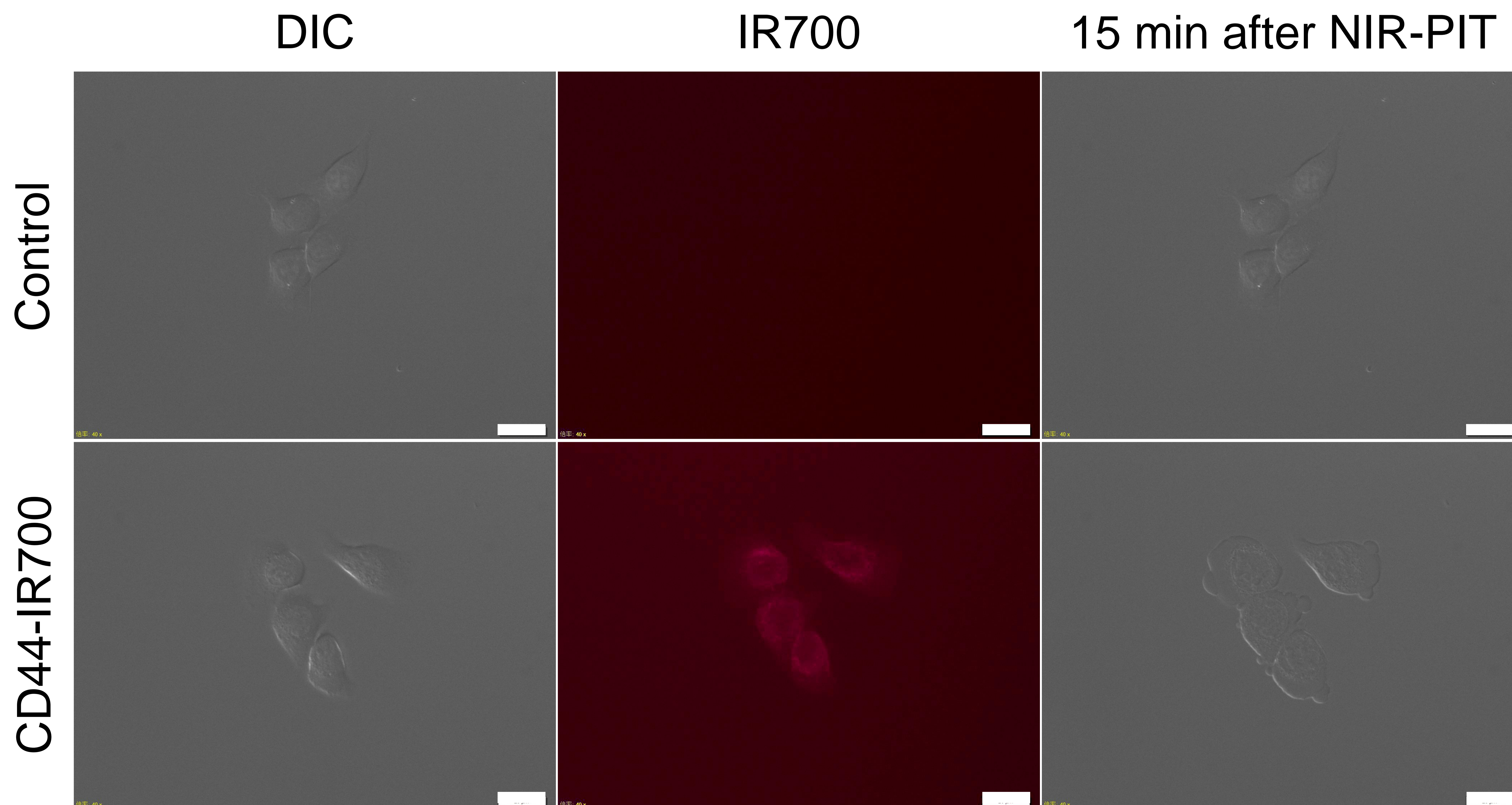
C



A



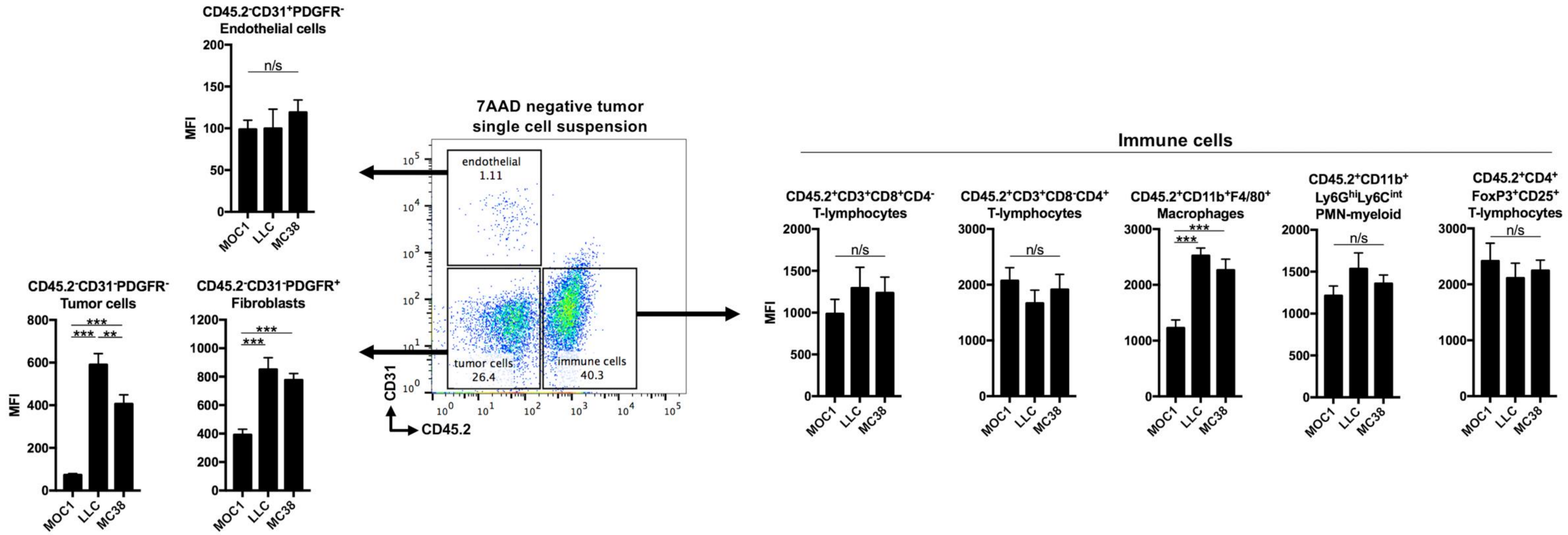
B



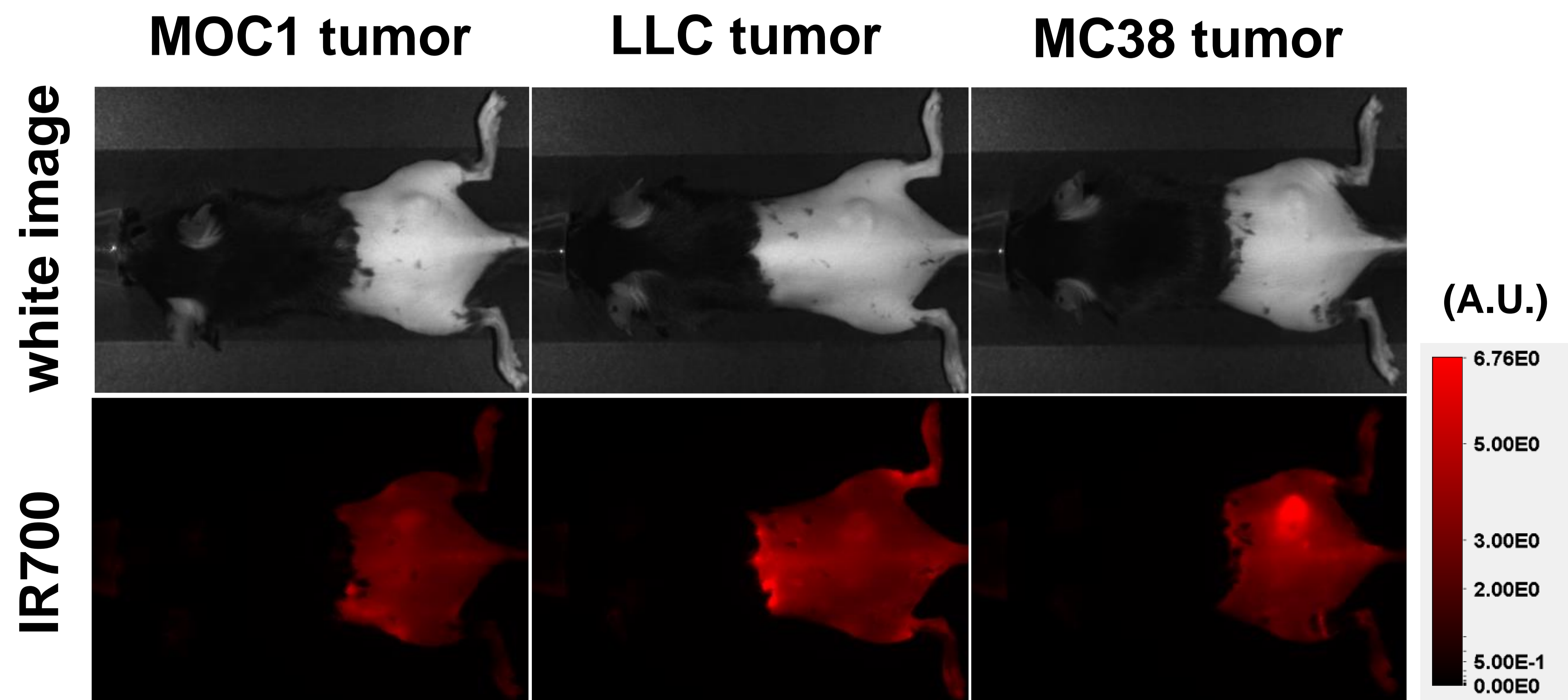
Supplementary Figure 2. Confirmation of CD44 expression as a target for NIR-PIT in MOC1 cells and evaluation of *in vitro* NIR-PIT.

(A) Expression of cell surface CD44 in MOC1 cells was examined with flow cytometry. CD44 blocking antibody was added to some wells to validate specific staining. Representative histograms shown. (B) DIC and fluorescence microscopy images of MOC1 cells. Change in MOC1 cellular architecture following 15 min of NIR light exposure shown. Scale bars = 20 μm . (C) Membrane permeability of MOC1 cells, as measured by PI staining, after labeling with CD44-IR700 and treatment with NIR-light (n = 5, * $p < 0.05$, ** $p < 0.01$, vs untreated control, by Student's t test).

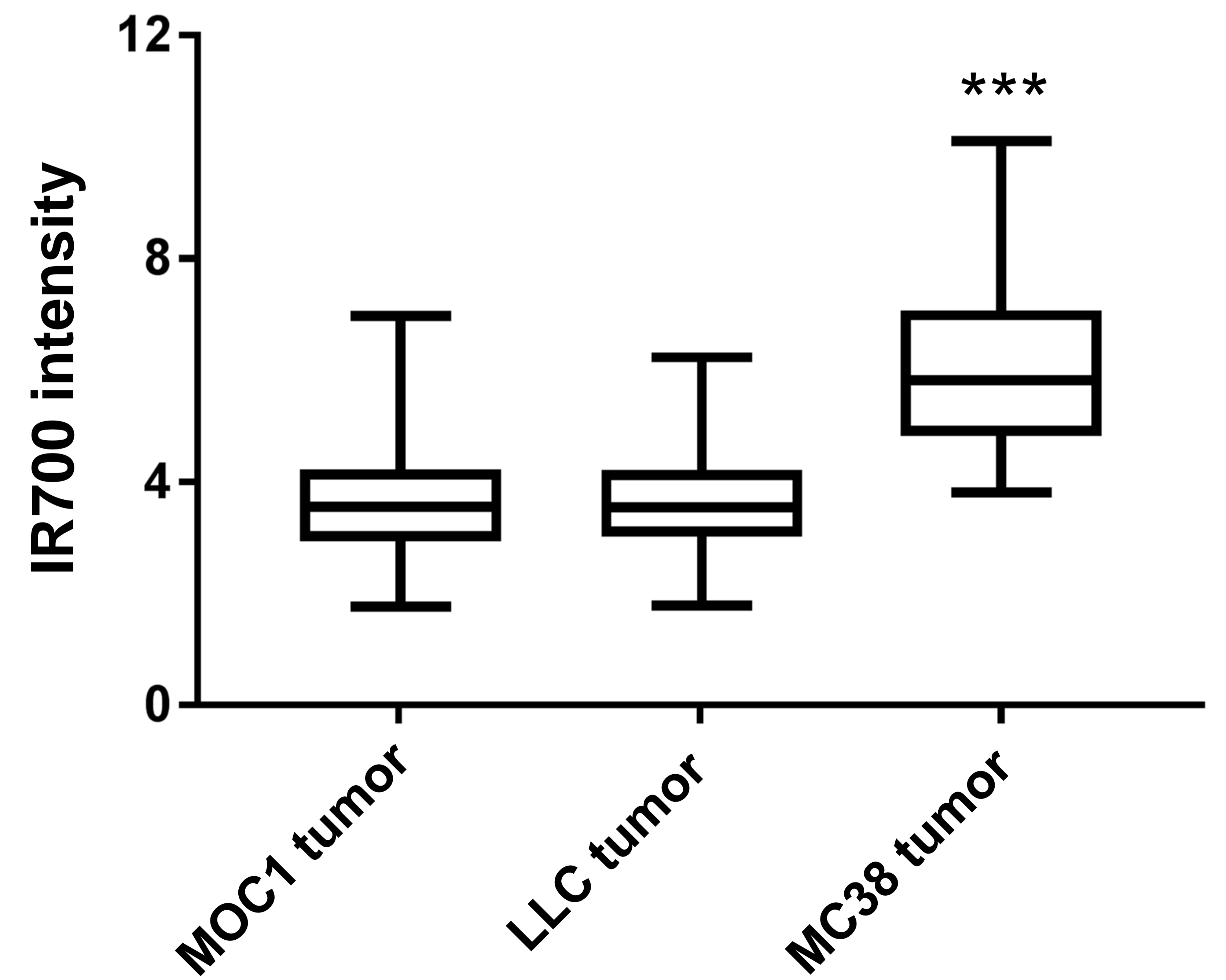
A



B



C

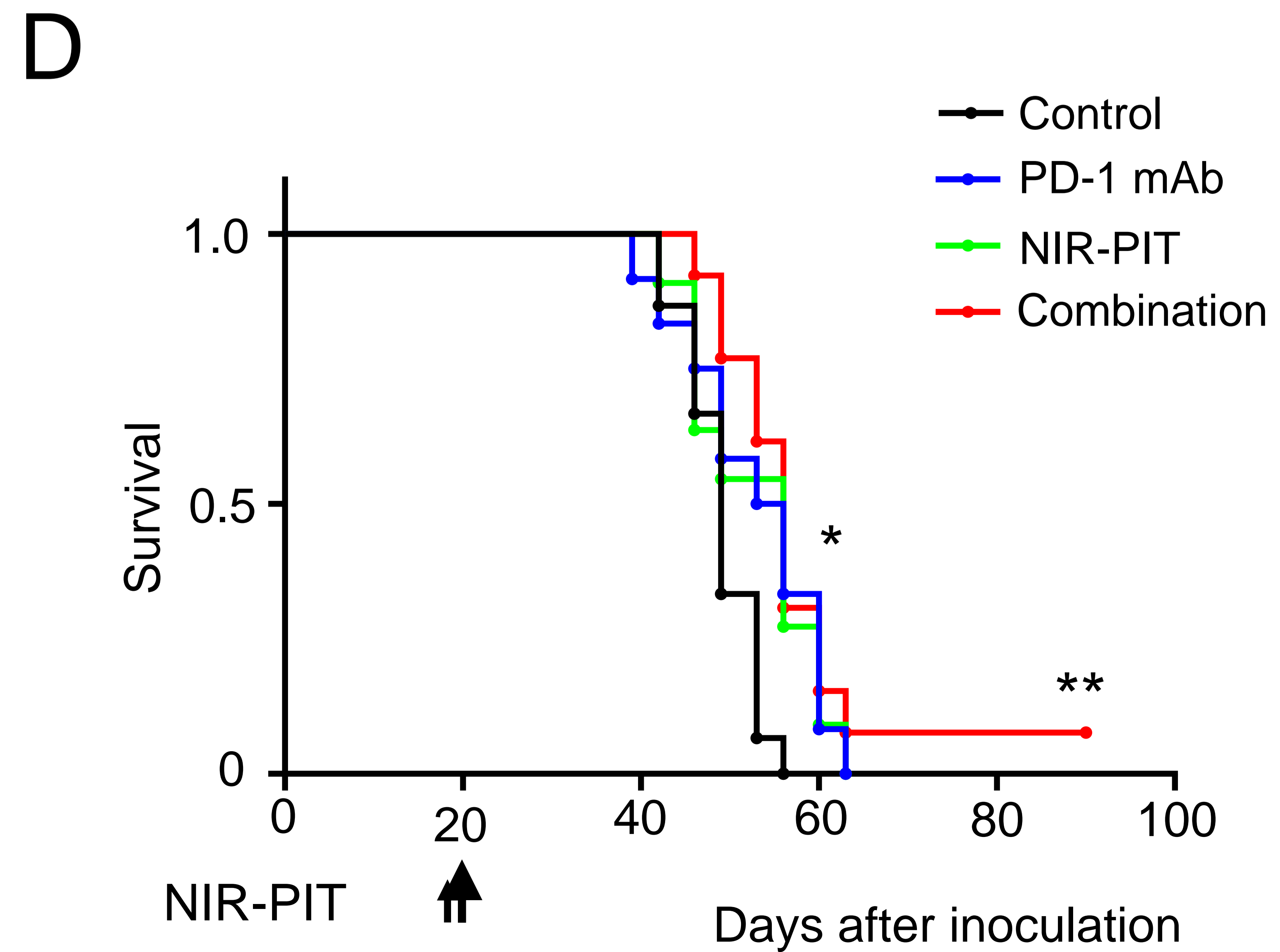
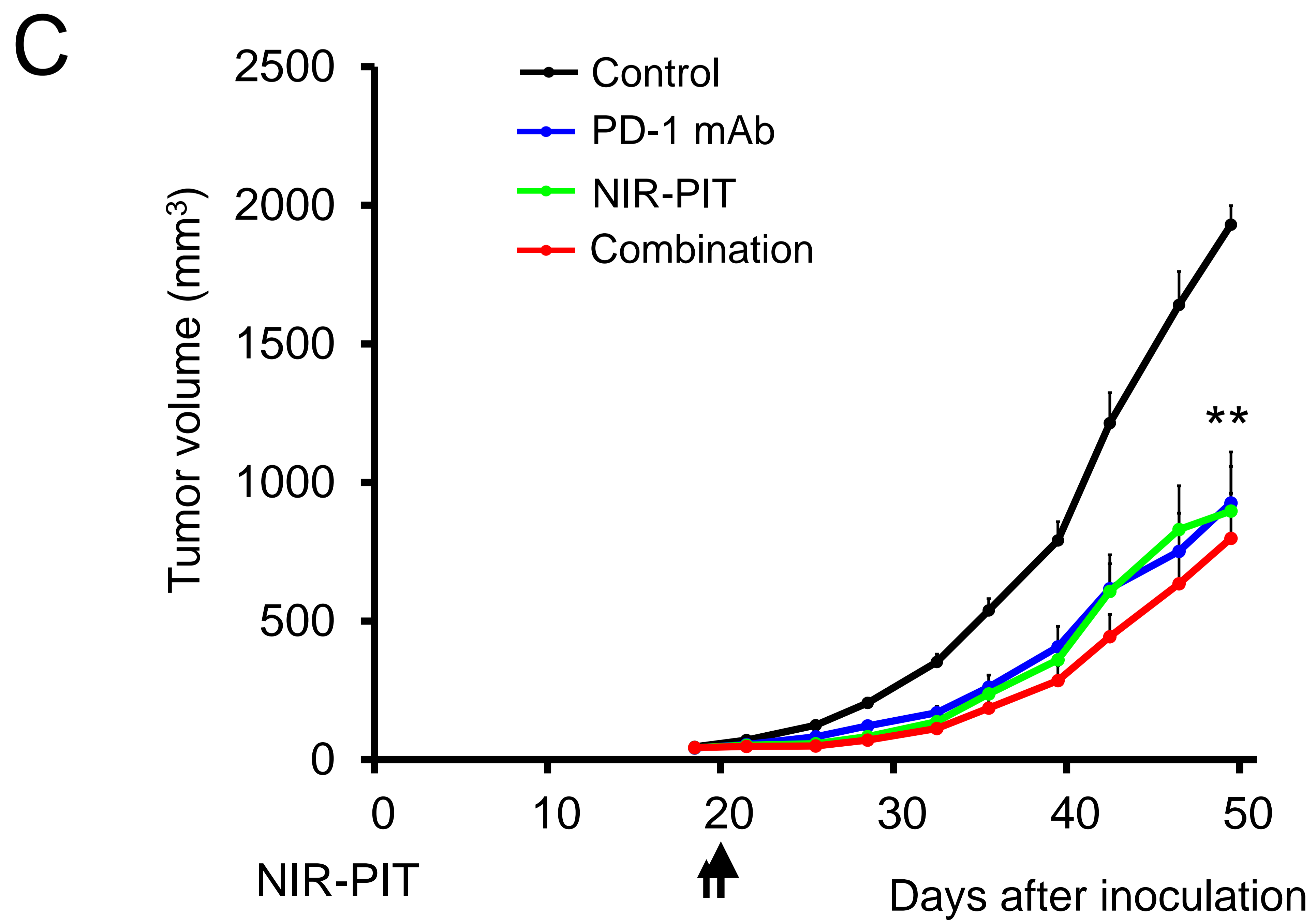
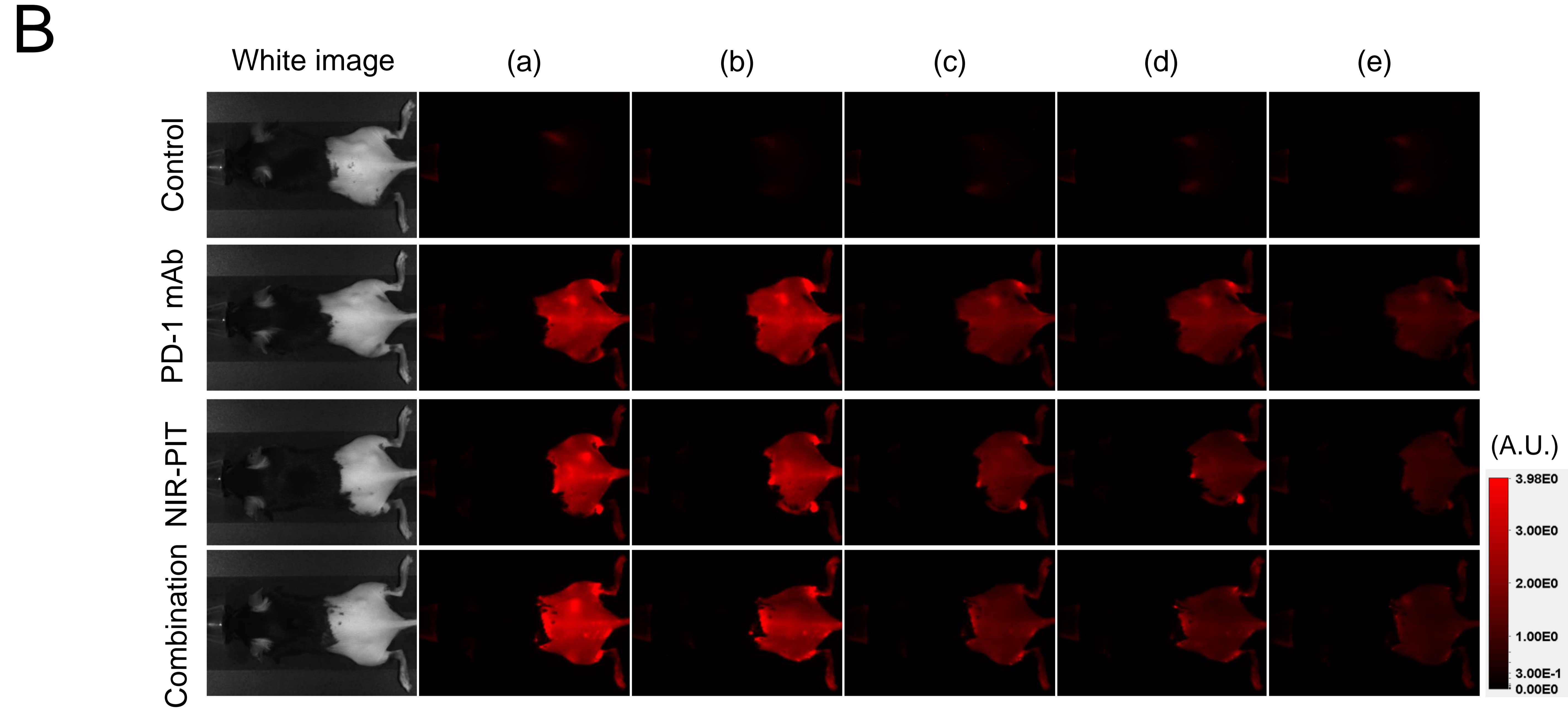
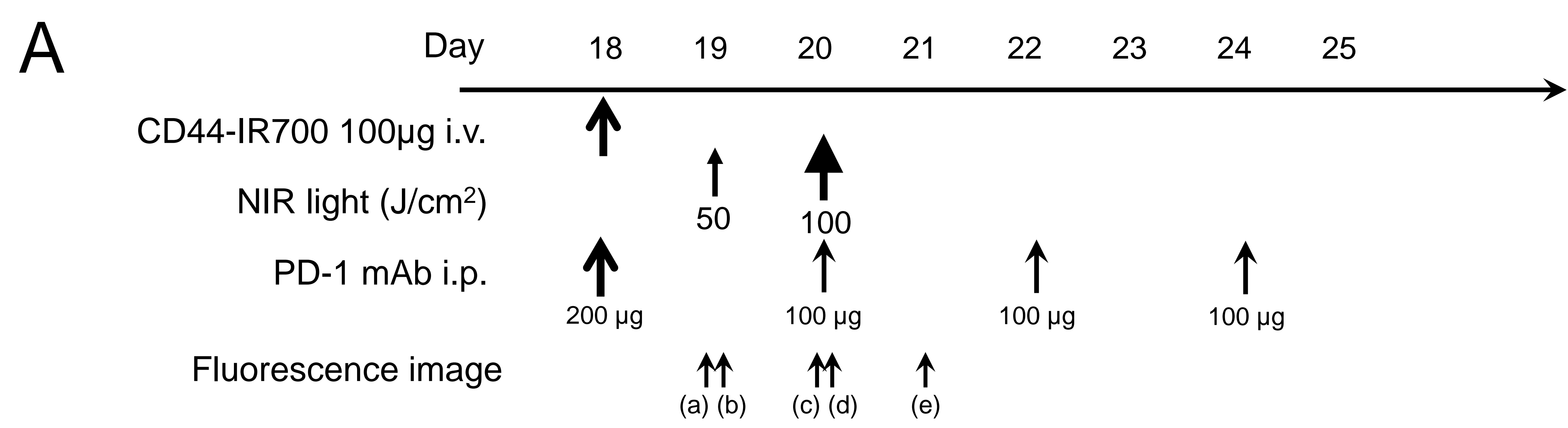


Supplementary Figure 3. Baseline CD44 expression within MOC1, LLC and MC38-luc tumor compartments.

(A) Size matched MOC1 (day 24), LLC (day 10) and MC38-luc (day 10) tumors were harvested digested into a single cell suspension, and assessed for CD44 expression on individual cell types via flow cytometry (n = 3/group). Representative dot plot and gating strategy of a tumor digest shown. Cell surface phenotype of each cell type shown above bar graphs. $**p < 0.01$, $***p < 0.001$, t test with ANOVA. (B) *In vivo* CD44-IR700 fluorescence real-time imaging of tumor bearing mice. Images were obtained of MOC1 (day 18), LLC (day 4) and MC38-luc (day 4) tumors 24 hours after i.v. injection of CD44-IR700. The fluorescence intensity of CD44IR-700 was higher in MC38 tumor compared with the other two tumors. (C) Quantitative analysis of IR700 intensities in MOC1, LLC and MC38-luc tumors. The fluorescence intensities were significantly higher in MC38-luc tumors compared with other tumors (n \geq 10, $***p < 0.001$ vs MOC1 and LLC tumor, Tukey's test with ANOVA).

Supplementary Figure 4. *In vivo* effect of NIR-PIT and PD-1 mAb in mice bearing a unilateral LLC tumor.

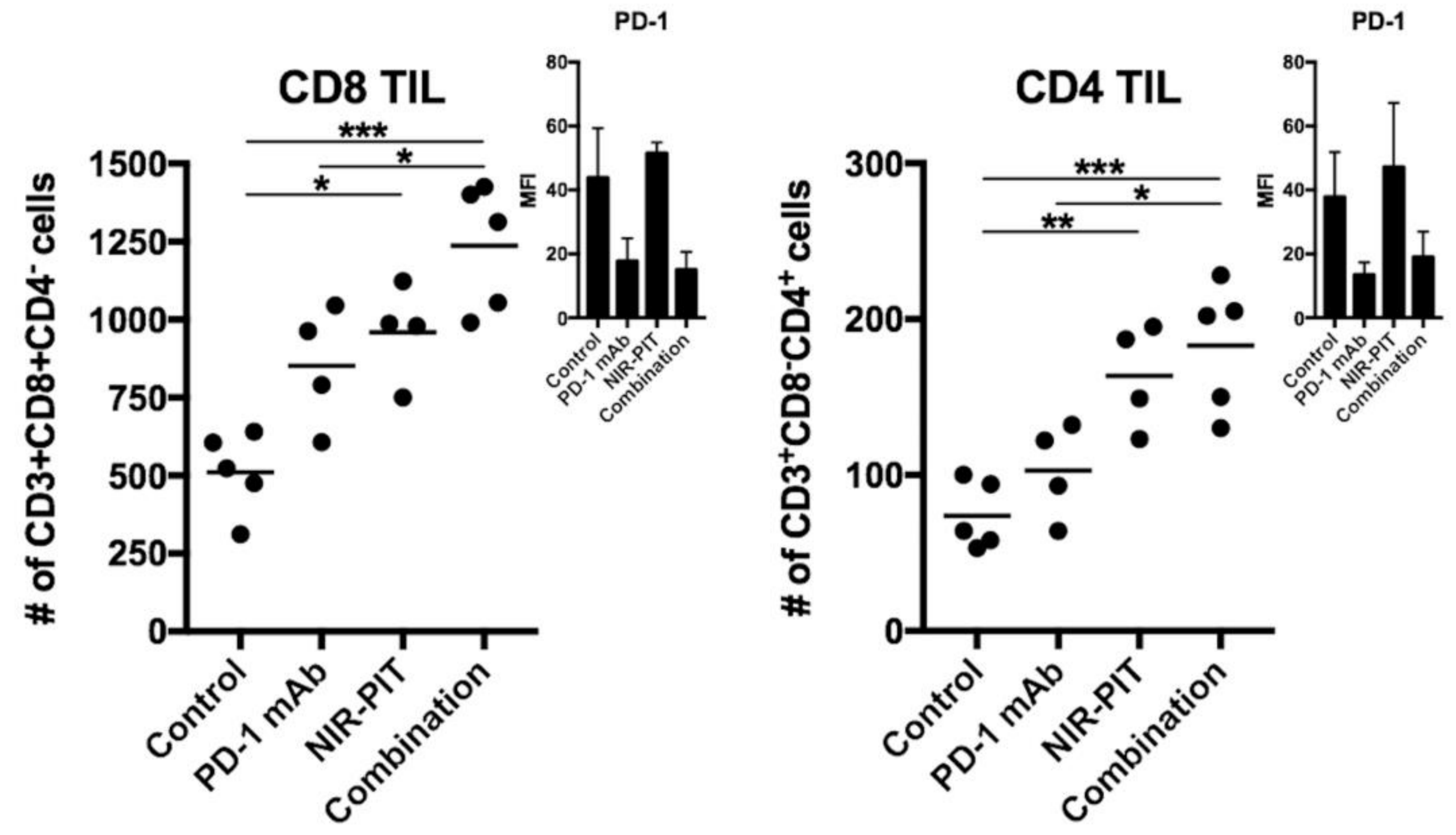
(A) NIR-PIT regimen. Bioluminescence and fluorescence images were obtained at each time point as indicated. (B) *In vivo* IR700 fluorescence real-time imaging of tumor-bearing mice in response to NIR-PIT alone or in combination with PD-1 mAb. Mice in the PD-1 mAb group also received CD44-IR700 but were not treated with NIR. (C) LLC tumor growth curves following NIR-PIT treatment with and without PD-1 mAb ($n \geq 10$, $**p < 0.01$ vs control, $^{##}p < 0.01$ vs PD-1 mAb and NIR-PIT groups, Tukey's t test with ANOVA). (D) Kaplan-Meier survival analysis ($n \geq 10$, $*p < 0.05$, $**p < 0.01$ vs control, $^{##}p < 0.01$ vs PD-1 mAb and NIR-PIT groups, Log rank test).



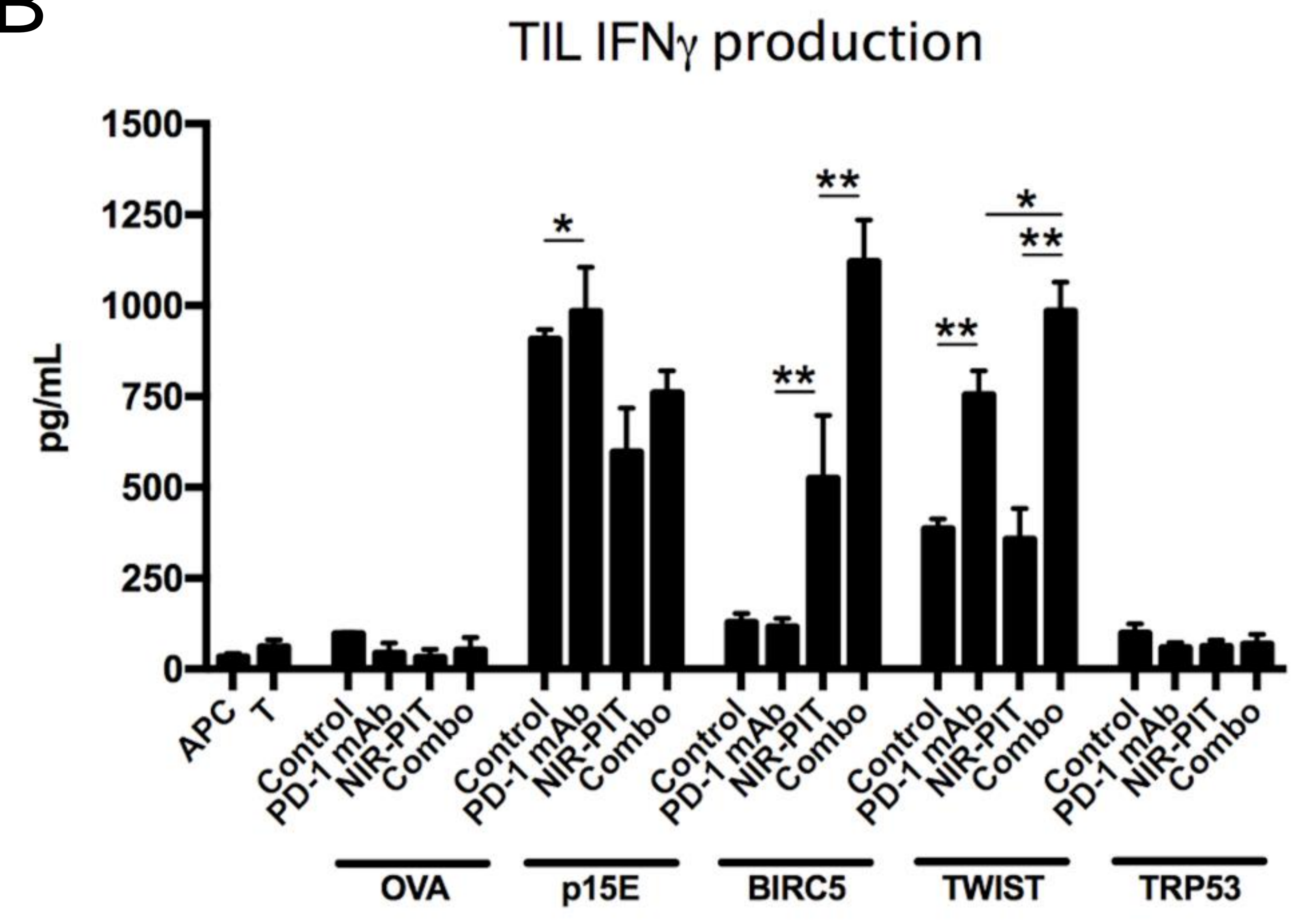
Supplementary Figure 5. *In vivo* effect of NIR-PIT and PD-1 mAb in mice bearing a unilateral MOC1 tumor.

(A) NIR-PIT regimen. Bioluminescence and fluorescence images were obtained at each time point as indicated. (B) *In vivo* IR700 fluorescence real-time imaging of tumor-bearing mice in response to NIR-PIT alone or in combination with PD-1 mAb. Mice in the PD-1 mAb group also received CD44-IR700 but were not treated with NIR. (C) MOC1 tumor growth curves following NIR-PIT treatment with and without PD-1 ($n \geq 10$, $**p < 0.01$ vs control, Tukey's test with ANOVA). (D) Kaplan-Meier survival analysis ($n \geq 10$, $*p < 0.05$, $**p < 0.01$ vs control, Log rank test).

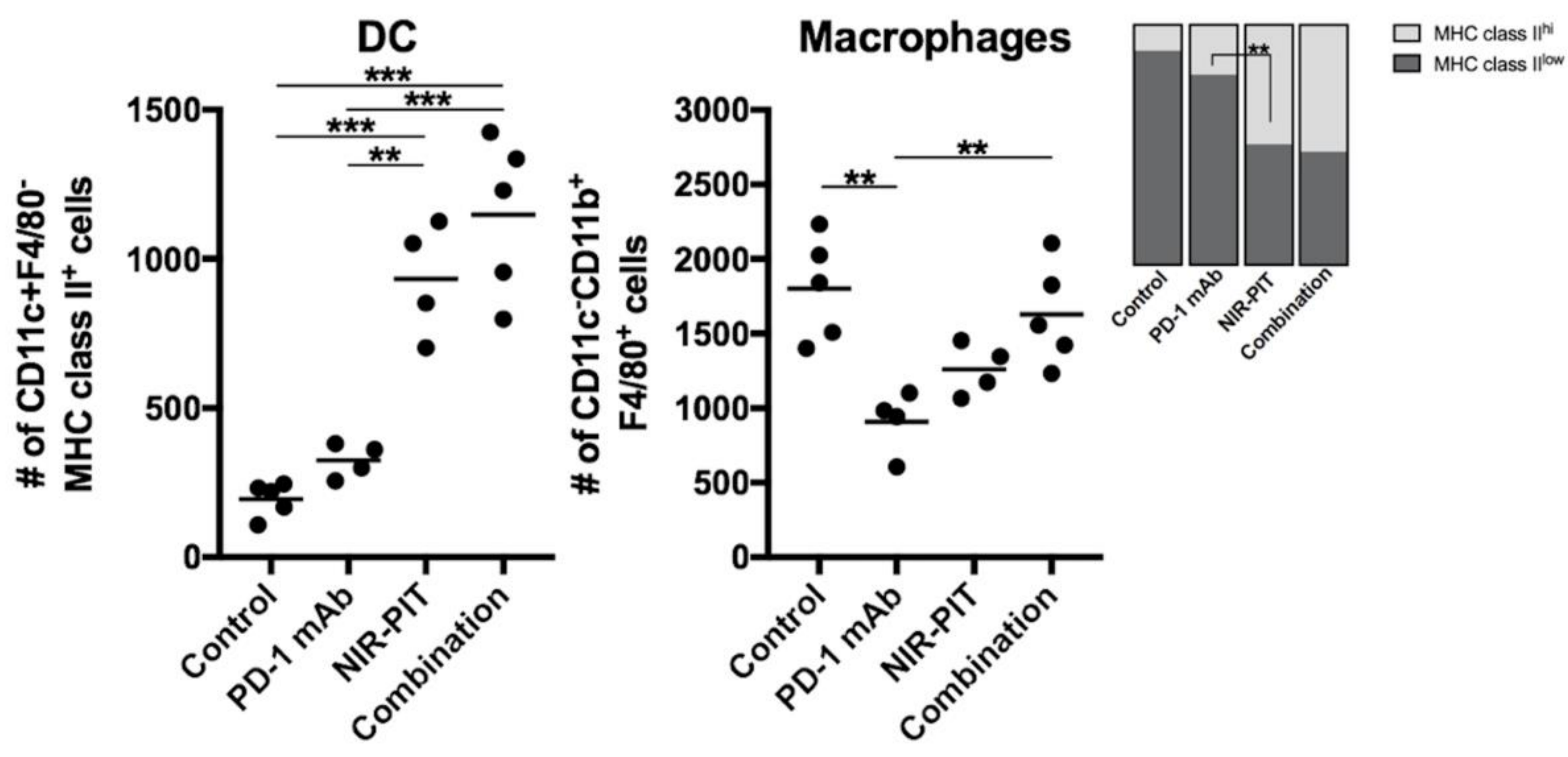
A



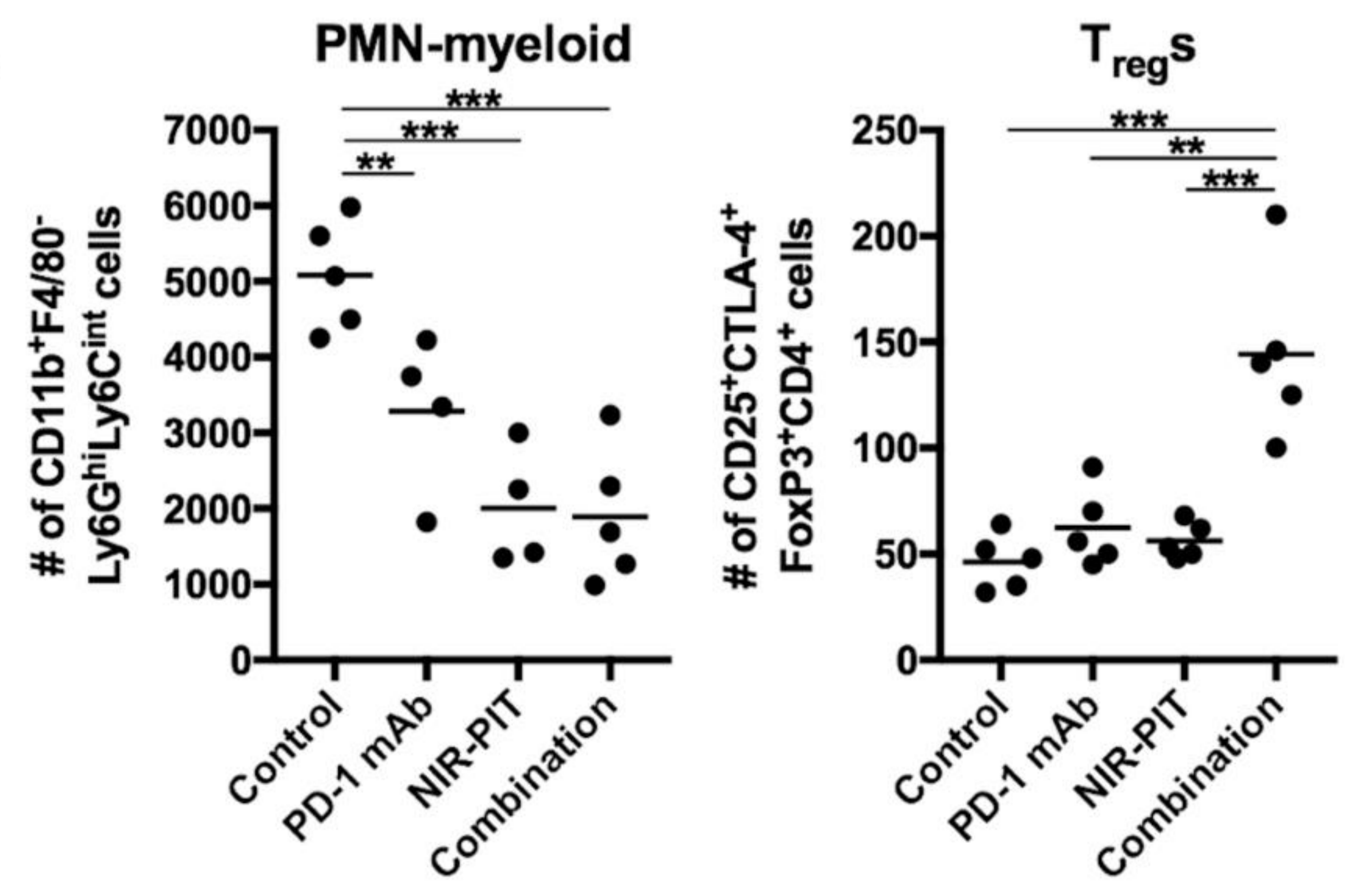
B



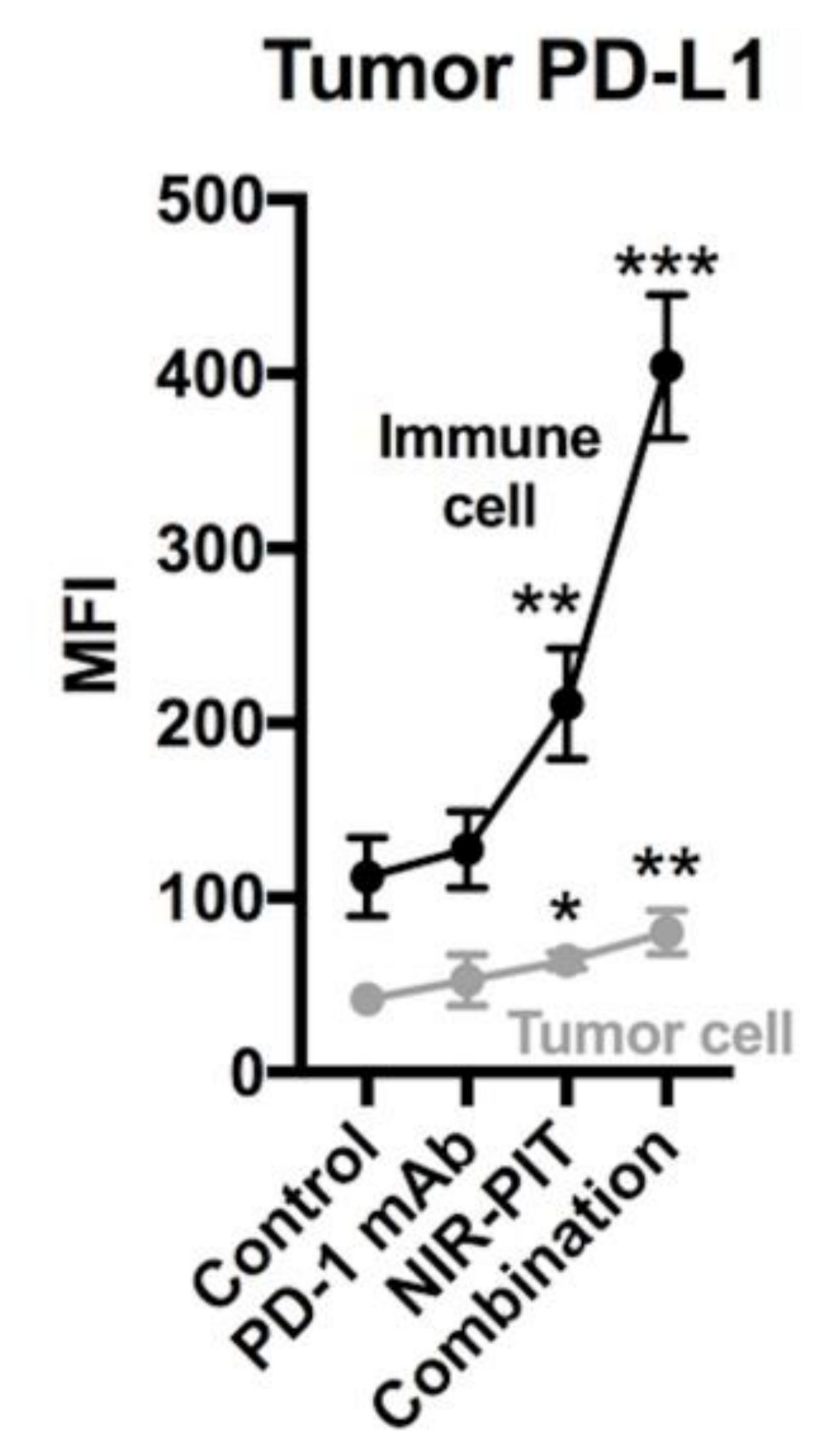
C



D



E

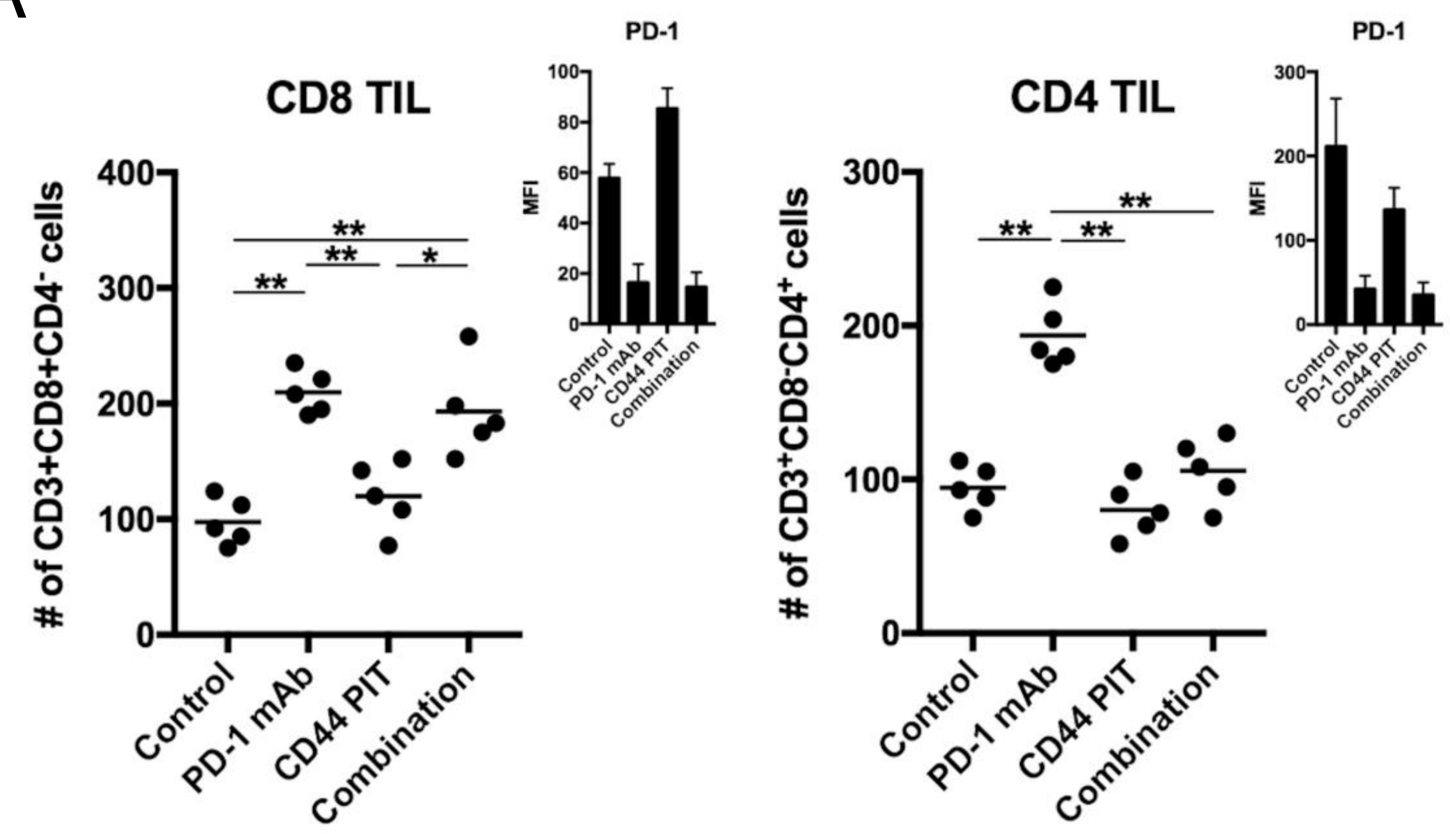


Supplementary Figure 6. Immune correlative and functional effects of NIR-PIT and PD-1 mAb in mice bearing a unilateral LLC tumor.

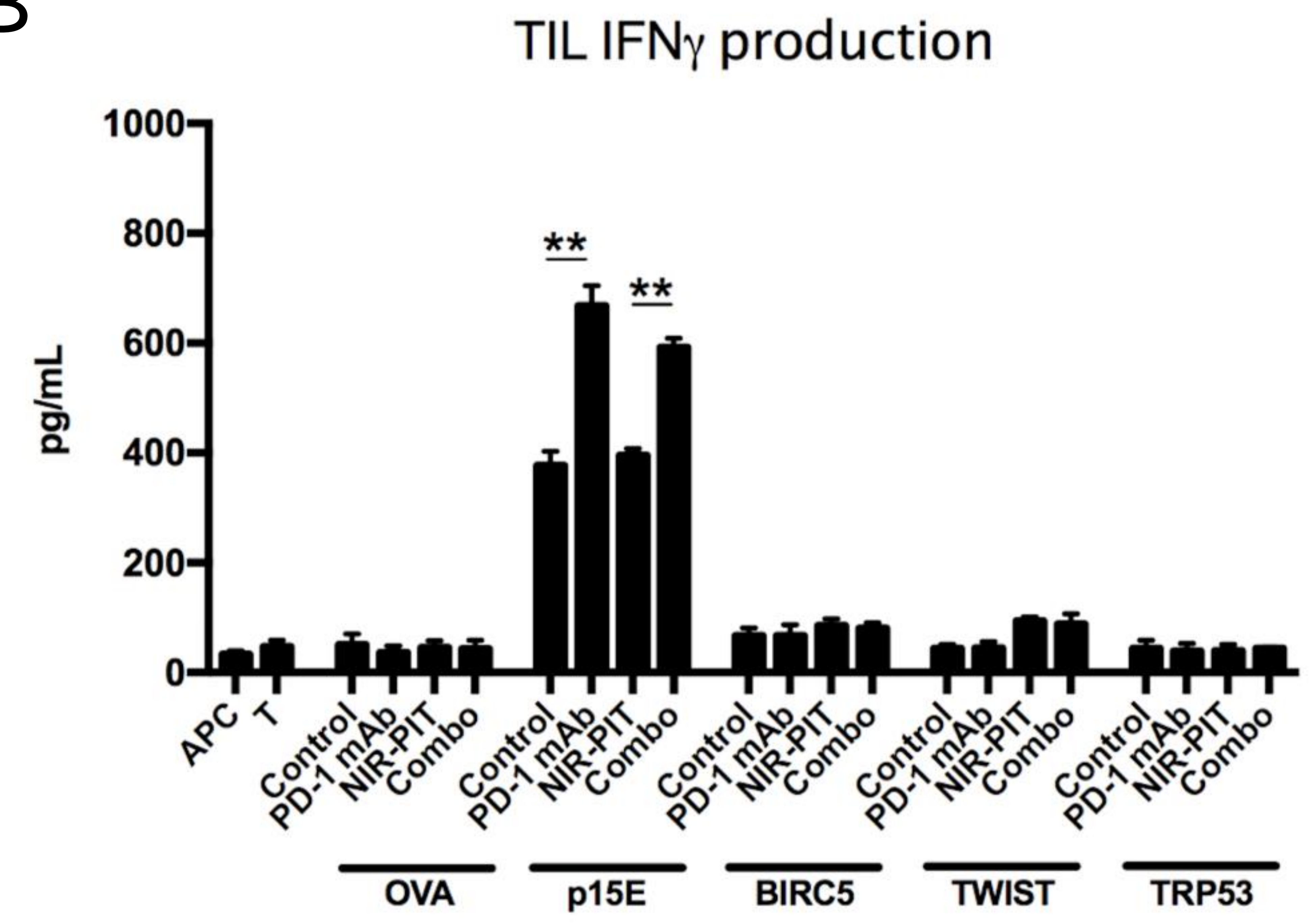
(A) LLC tumors (day 10, n = 5/group) treated with NIR-PIT with and without systemic PD-1 mAb and controls were harvested, digested into single-cell suspensions, and analyzed for tumor infiltrating lymphocytes (TIL) infiltration via flow cytometry. Presented as absolute number of infiltrating cells per 1.5×10^4 live cells analyzed. PD-1 expression shown as inset (MFI, mean fluorescence intensity). * $p < 0.05$, ** $p < 0.01$, *** $p < 0.001$, t test with ANOVA. (B) TIL were extracted from tumors treated as above (n = 5/group) via an IL-2 gradient, enriched via negative magnetic selection, and stimulated with irradiated splenocytes pulsed with peptides representing known MHC class I-restricted epitopes from selected tumor-associated antigens. IFN γ levels determined by ELISA from supernatants collected 24 hours after stimulation. Supernatants from splenocytes (APC) alone, TIL (T) alone, and a MHC-class I-restricted epitope from ovalbumin (OVA, SIINFEKL) used as controls. * $p < 0.05$, ** $p < 0.01$, t test with ANOVA. (C) Flow cytometric analysis of tumor infiltrating dendritic cells (DC) and macrophages, with quantification of macrophage polarization

based on MHC class II expression. $**p < 0.01$, $***p < 0.001$, t test with ANOVA. (E) Flow cytometric analysis of tumor infiltrating granulocytic myeloid derived suppressor cells PMN-myeloid and T_{reg}S. $**p < 0.01$, $***p < 0.001$, t test with ANOVA. (F) Flow cytometric analysis of PD-L1 expression on CD45.2⁻CD31⁻PDGFR⁻ tumor cells and CD45.2⁺CD31⁻ immune cells. N = 5/group. $*p < 0.05$, $**p < 0.01$, $***p < 0.001$, t test with ANOVA.

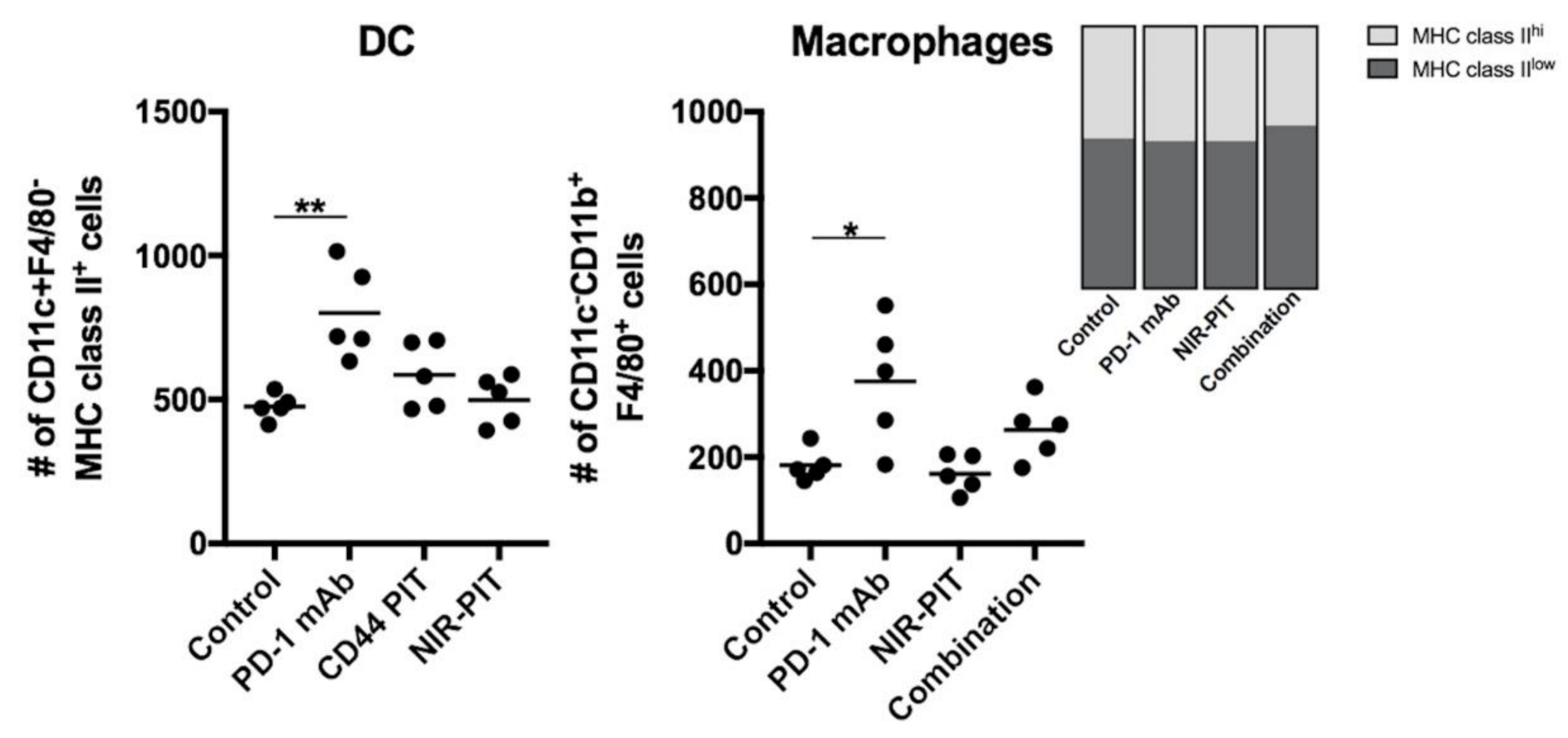
A



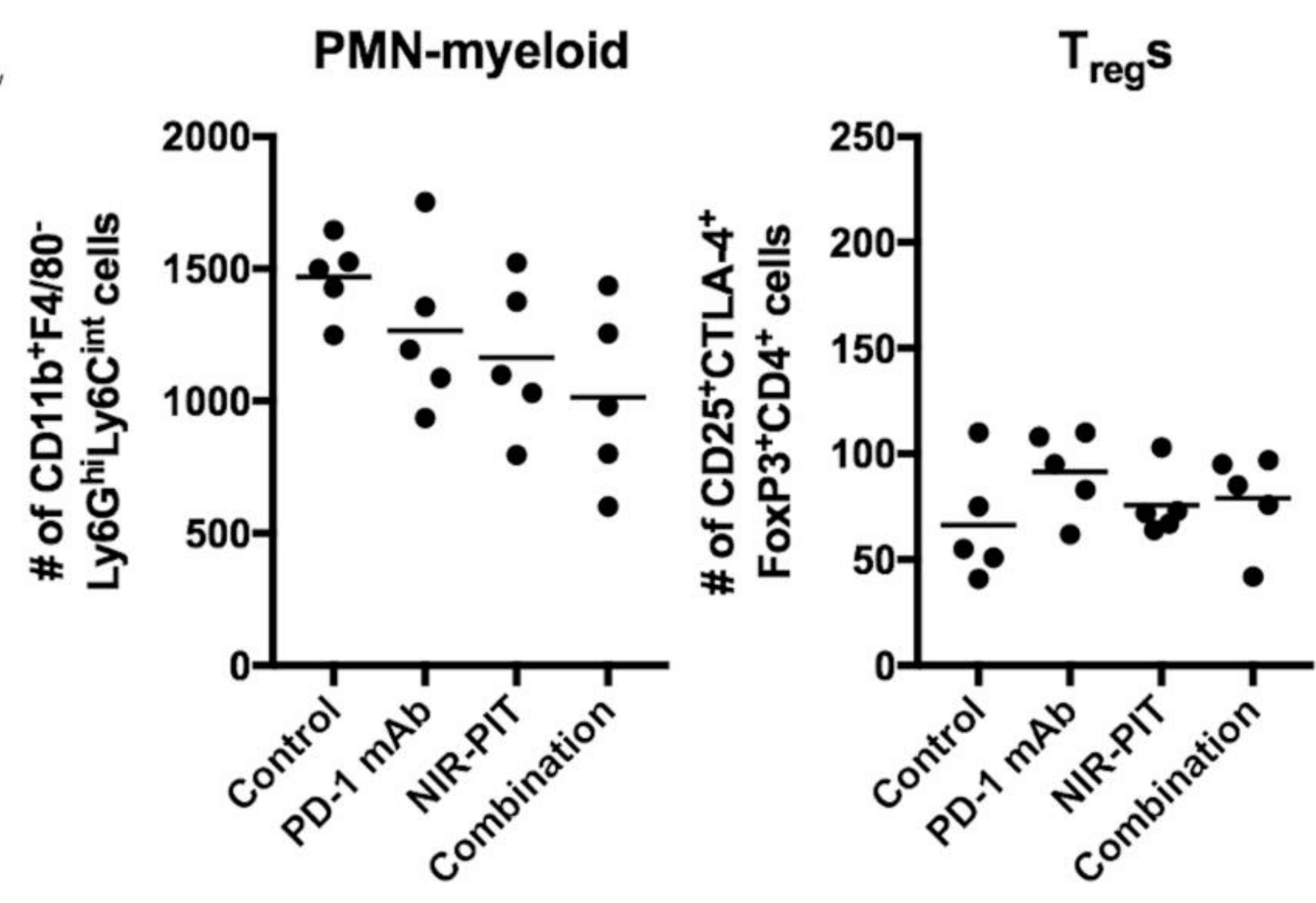
B



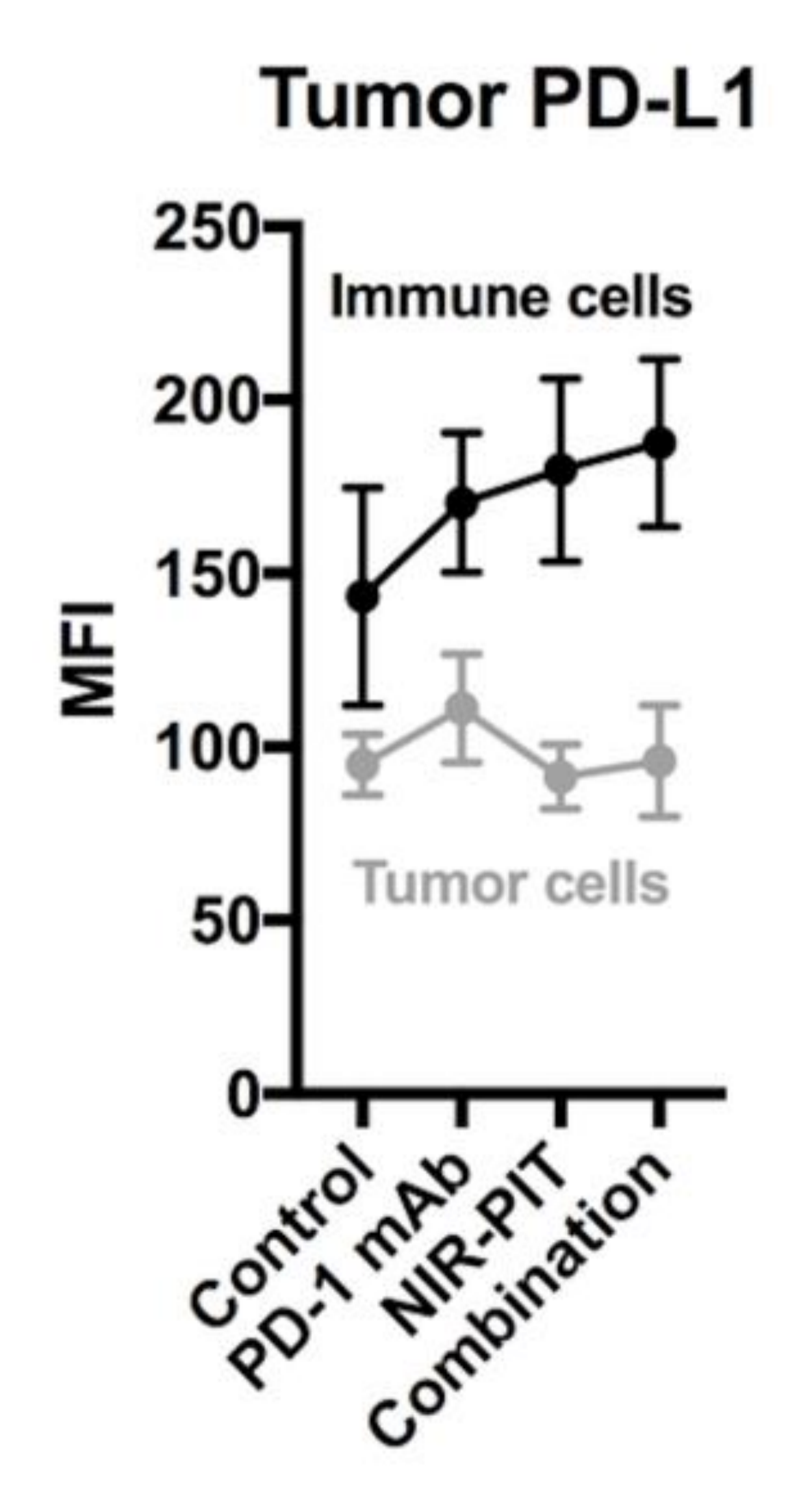
C



D



E



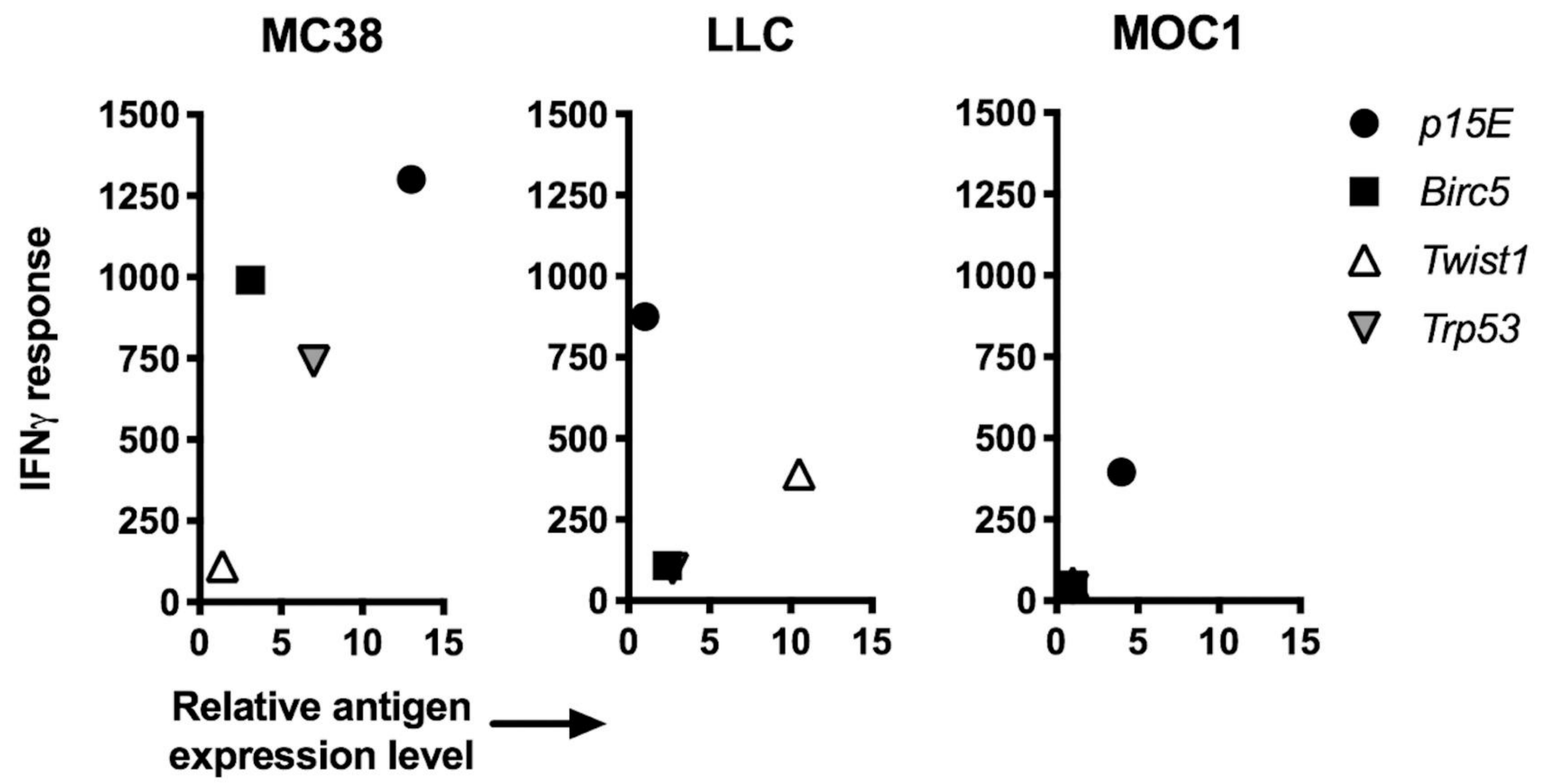
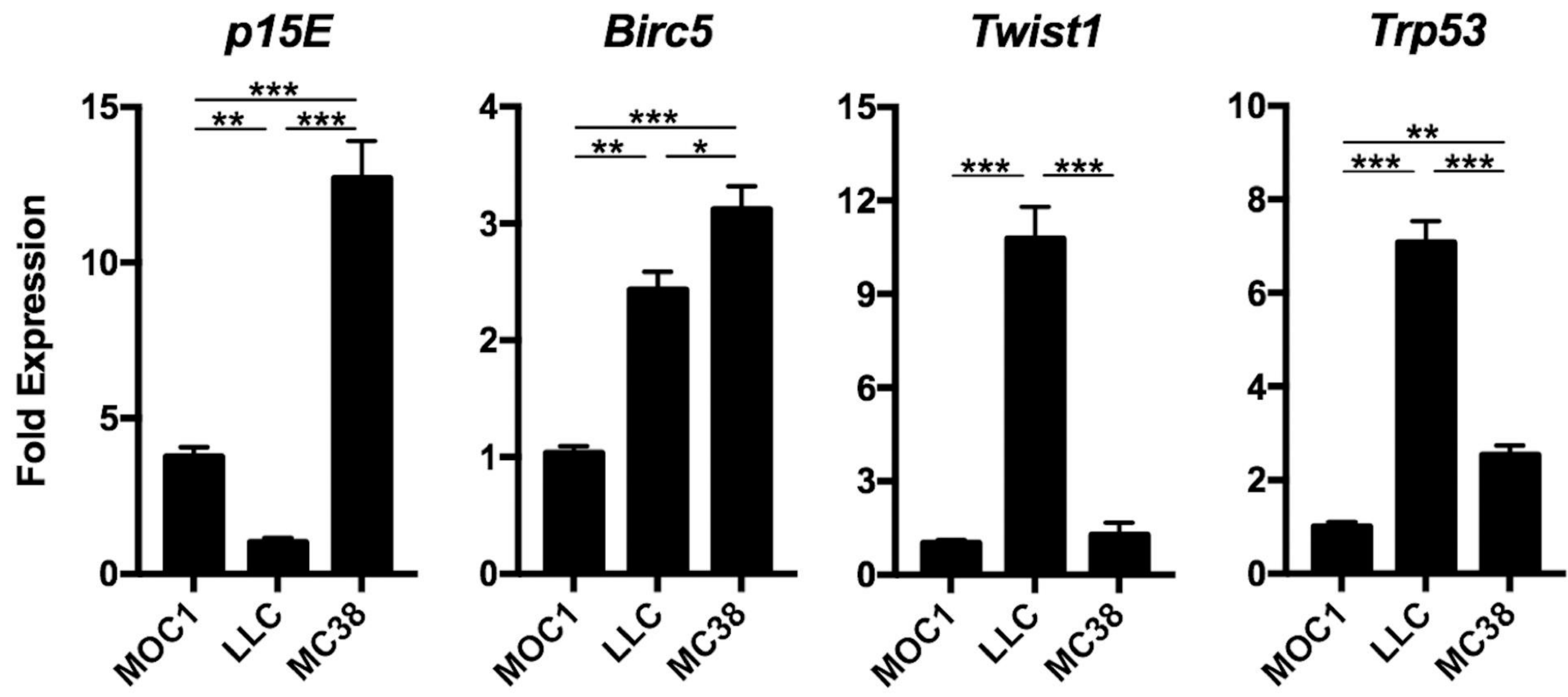
Supplementary Figure 7. Immune correlative and functional effects of NIR-PIT and PD-1 mAb in MOC1 tumor-bearing mice.

(A) MOC1 tumors (day 10, n = 5/group) treated with NIR-PIT with and without systemic PD-1 mAb and controls were harvested, digested into single-cell suspensions, and analyzed for tumor infiltrating lymphocytes (TIL) infiltration via flow cytometry. Presented as absolute number of infiltrating cells per 1.5×10^4 live cells analyzed. PD-1 expression shown as inset (MFI, mean fluorescence intensity). * $p < 0.05$, ** $p < 0.01$, t test with ANOVA. (B) TIL were extracted from tumors treated as above (n = 5/group) via an IL-2 gradient, enriched via negative magnetic selection, and stimulated with irradiated splenocytes pulsed with peptides representing known MHC class I-restricted epitopes from selected tumor-associated antigens. IFN γ levels determined by ELISA from supernatants collected 24 hours after stimulation. Supernatants from splenocytes (APC) alone, TIL (T) alone, and a MHC-class I-restricted epitope from ovalbumin (OVA, SIINFEKL) used as controls. ** $p < 0.01$, t test with ANOVA. (C) Flow cytometric analysis of tumor infiltrating dendritic cells (DC) and macrophages, with quantification of macrophage polarization based on

MHC class II expression. $*p < 0.05$, $**p < 0.01$, t test with ANOVA. (D)

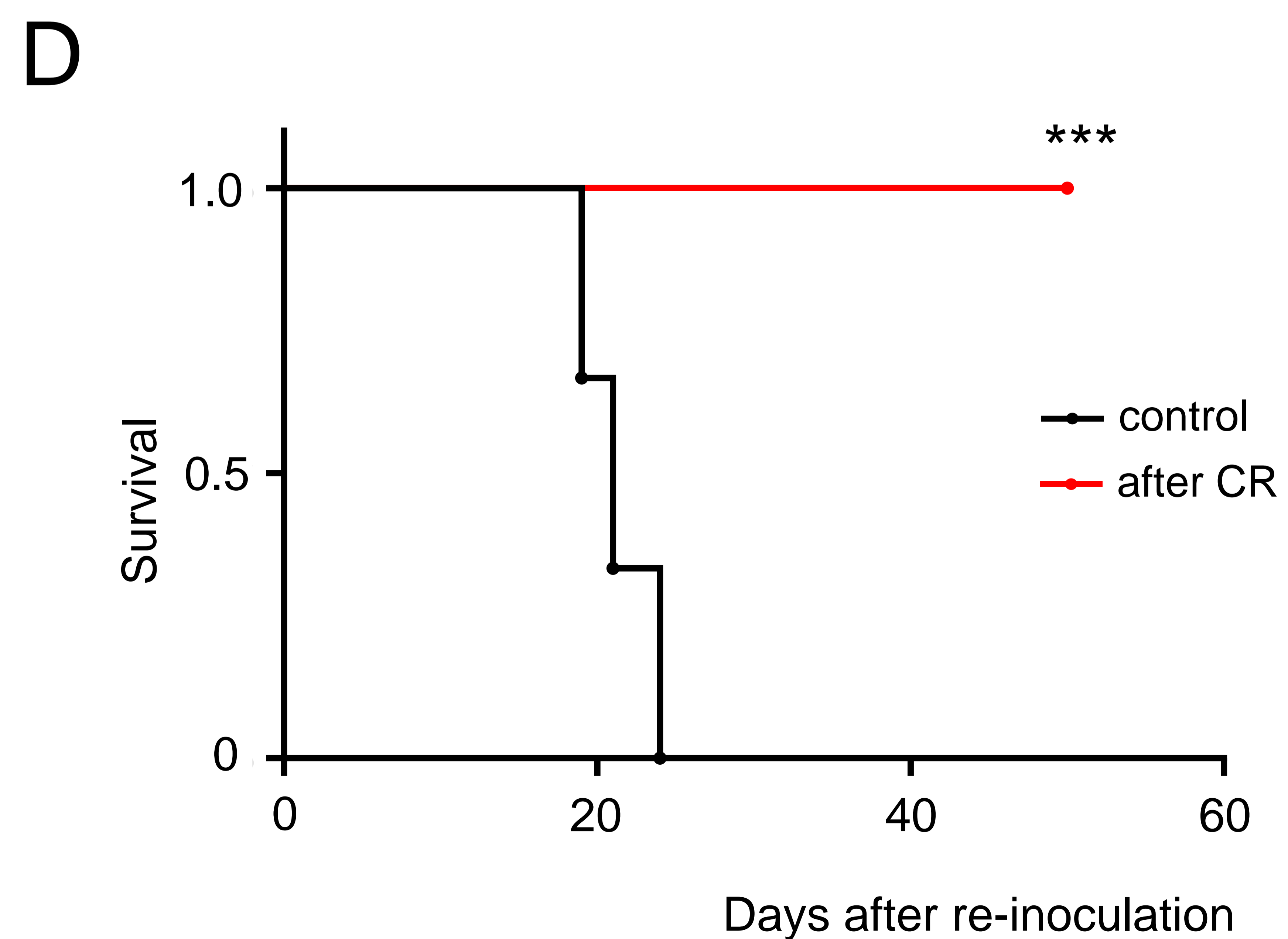
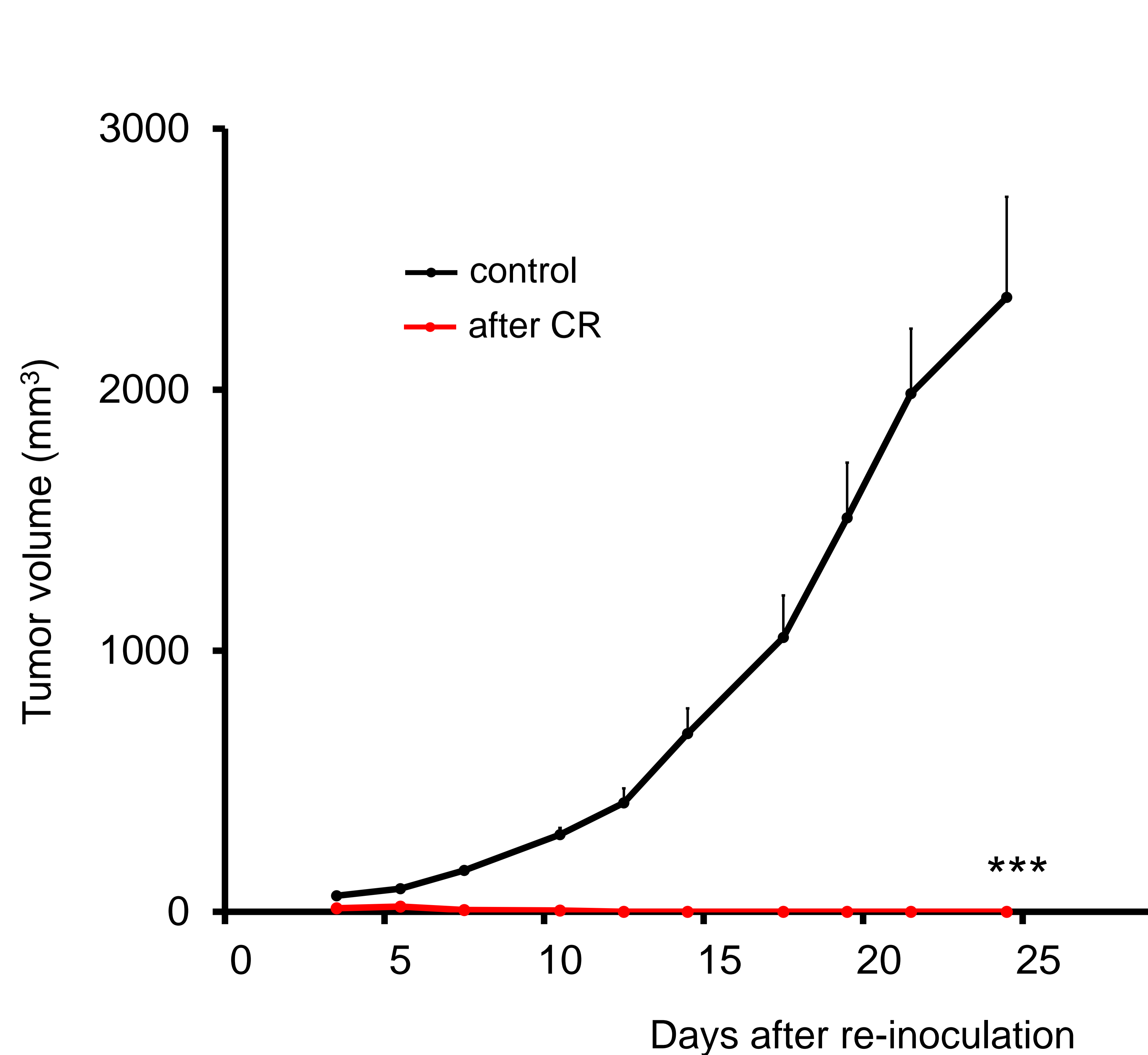
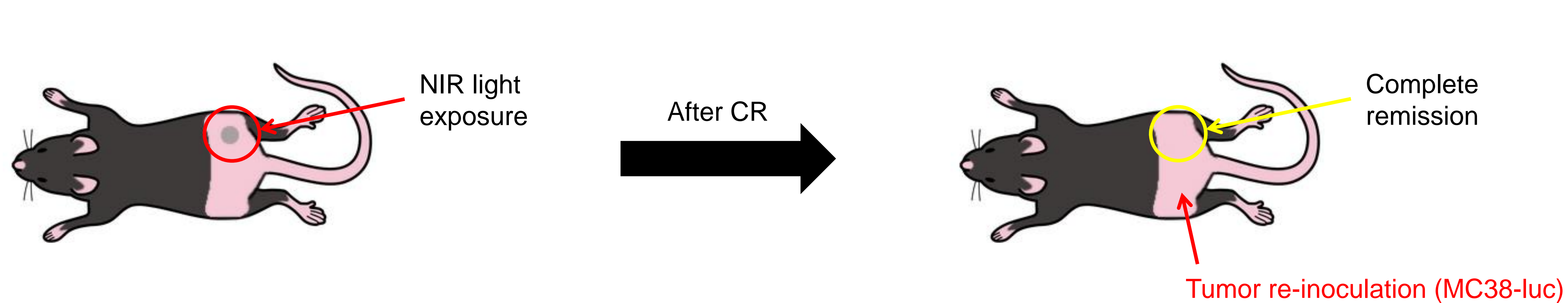
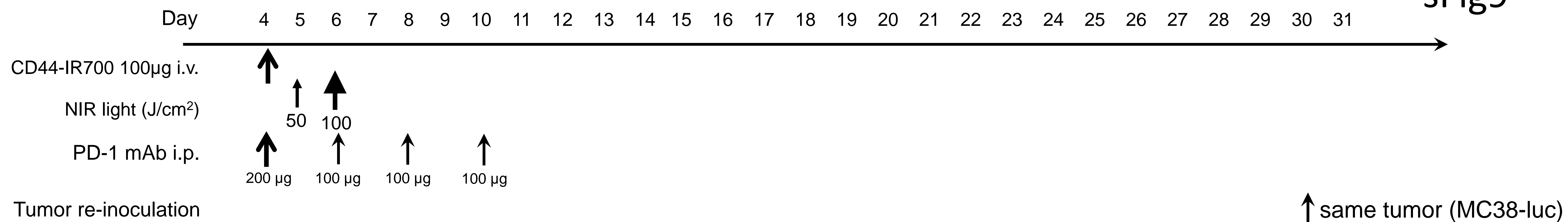
Flow cytometric analysis of tumor infiltrating PMN-myeloid and T_{reg}S. (E)

Flow cytometric analysis of PD-L1 expression on CD45.2⁻CD31⁻PDGFR⁻ tumor cells and CD45.2⁺CD31⁻ immune cells. N = 5/group.



Supplementary Figure 8. Relative tumor associated antigen gene expression.

MC38-luc, LLC and MOC1 cells were processed and assessed for gene expression of *p15E*, *Birb5*, *Twist1* and *Trp53* by qRT-PCR using custom primers designed to flank the region encoding the MHC class I-restricted epitope ($*p < 0.05$, $**p < 0.01$, $***p < 0.001$, t test with ANOVA.). Two-dimensional plot of relative antigen expression level vs baseline antigen-specific IFN γ responses in TIL for each model shown on bottom.



Supplementary Figure 9. Resistance to re-challenge with MC38-luc cells following complete tumor rejection with combination NIR-PIT and PD-1 mAb treatment

(A) The regimen of tumor re-challenge in mice that completely rejected (CR) tumors with combination treatment. Tumor was inoculated on the contralateral side 30 days after first inoculation. (B) Mice receiving re-inoculation of MC38-luc cells. (C) Growth curves of control and CR mice challenged with MC38-luc cells in the contralateral flank. (D) Kaplan-Meier survival analysis ($n = 9$, $***p < 0.001$, by Tukey's test with ANOVA for growth curves, $***p < 0.001$, by Log-rank test for survival).

Supplementary Videos

1 - 3

Supplementary Video 1:

Microscopic image of *in vitro* NIR-PIT for MC38 cell

Supplementary Video 2:

Microscopic image of *in vitro* NIR-PIT for LLC cell

Supplementary Video 3:

Microscopic image of *in vitro* NIR-PIT for MOC1 cell